JOURNAL OF GEOPHYSICAL RESEARCH, VOL. 111, C03S12, doi:10.1029/2006JC003511, 2006 [printed 112(C3), 2007]

Simulation of the northern Adriatic circulation during winter 2003

P. J. Martin,[1] J. W. Book,[2] and J. D. Doyle[3]

Received 30 January 2006; revised 18 May 2006; accepted 3 July 2006; published 19 December 2006.

[1] Numerical simulations of the Adriatic Sea were conducted with the Navy Coastal Ocean Model during the Adriatic Circulation Experiment in the fall and winter of 2002/2003, and results were compared with observations. The ocean model used a 1-km resolution grid over the entire Adriatic Sea. Model forcing included atmospheric fluxes from the Coupled Ocean-Atmosphere Mesoscale Prediction System (COAMPS), tides, boundary conditions from a global model, and freshwater river and runoff inflows. Model tidal elevation showed good agreement with International Hydrographic Organization station data, and model tidal currents showed good agreement with tidal currents determined from acoustic Doppler current profiler (ADCP) measurements. Detided model currents showed good agreement with ADCP currents with rms errors along the principal variance axes ranging from 6 to 12.9 cm/s and correlations ranging from 0.16 to 0.81. Correlations between model and ADCP currents along the minor variance axes were generally low. Comparison of the model-simulated temperature and salinity profiles during January and February with conductivity-temperature-depth measurements indicated that the model captured some of the spatial structure of the observed fields. The model response to several bora wind events in January and February showed a recurring pattern of cyclonic and anticyclonic gyres that generally agreed with observations and reflected the pattern of wind stress curl from the COAMPS wind stress forcing. During strong bora forcing, two large cyclonic circulation gyres form in the northern Adriatic with a smaller anticyclonic circulation between them near the Istrian Peninsula. Additionally, a couple of large meanders frequently occur within the Eastern Adriatic Current southeast of Kvarner Bay, and these meanders sometimes close to form small gyres.

Citation: Martin, P. J., J. W. Book, and J. D. Doyle (2006), Simulation of the northern Adriatic circulation during winter 2003, *J. Geophys. Res.*, *111*, C03S12, doi:10.1029/2006JC003511. [printed *112*(C3), 2007]

1. Introduction

[2] There has been a long-standing interest in theoretical and modeling studies of the Adriatic Sea as it is characterized by strong wind and river forcing and is a site of dense water formation for the eastern Mediterranean Sea [*Artegiani et al.*, 1997a, 1997b; *Cushman-Roisin et al.*, 2001].

[3] The general circulation of the Adriatic is cyclonic with southeastward flows along the western side of the sea and northwestward flows along the eastern side [*Orlic et al.*, 1992]. Three smaller cyclonic patterns are frequently observed within the overall cyclonic circulation [*Artegiani et al.*, 1997b; *Poulain*, 2001].

[4] In winter, the Adriatic is subject to a strong wind called a bora, which is a cold northeasterly wind that develops in the lee of the Dinaric Alps. A number of studies suggest that the bora shares some common characteristics with downslope windstorms and transcritical hydraulic flows [e.g., *Smith*, 1987; *Klemp and Durran*, 1987; *Jiang and Doyle*, 2005] The bora winds impact both the water characteristics and the circulation, especially in the shallow northern end of the Sea. The other primary wind pattern is the sirocco, which blows from the southeast along the axis of the Adriatic.

[5] There is a net gain of fresh water within the Adriatic Sea, unlike the Mediterranean as a whole. Total mean freshwater inflows into the Adriatic have been estimated to be about 5700 m^3/s [*Raicich*, 1994]. The largest single source of fresh water in the Adriatic is the Po River, which has an annual mean discharge of about 1500 m^3/s. This low-salinity water flows southeast along the Italian coast [*Hopkins et al.*, 1999] and joins a current turning to the southeast along the western Adriatic slope [*Zore-Armanda et al.*, 1996] to form the Western Adriatic Current (WAC). A less intense flow along the eastern side of the Adriatic forms the Eastern Adriatic Current (EAC).

[6] Past theoretical studies have been successful at describing the bulk features of the oceanography of the

[1]Ocean Dynamics and Prediction Branch, Oceanography Division, Naval Research Laboratory, Stennis Space Center, Mississippi, USA.
[2]Ocean Sciences Branch, Oceanography Division, Naval Research Laboratory, Stennis Space Center, Mississippi, USA.
[3]Atmospheric Dynamics and Prediction Branch, Marine Meteorology Division, Naval Research Laboratory, Monterey, California, USA.

Adriatic [e.g., *Hendershott and Rizzoli*, 1976; *Orlic et al.*, 1994]. However, recent numerical modeling studies have begun to focus on the more complicated details of the Adriatic, recognizing the importance of the fine scales of wind forcing [*Pullen et al.*, 2003] and using complex topography and models [*Beg Paklar et al.*, 2001; *Zavatarelli et al.*, 2002] to simulate more realistic conditions and study the prevailing dynamical details. Comparisons with data for these studies have been limited as most of the observations were confined to single point samples and were limited in spatial and temporal extent.

[7] An extensive international collaborative study of the northern and central Adriatic was conducted during the fall and winter of 2002/2003, which included a number of observational programs and numerical modeling efforts. Measurements that were made include acoustic Doppler current profilers (ADCPs), conductivity-temperature-depth (CTD) casts, surface drifter measurements, high-frequency radar measurements, meteorological platform and buoy measurements, towed body measurements, and other current mooring measurements [*Lee et al.*, 2005]. Numerical modeling efforts included high-resolution meteorological, ocean, wave, and sediment model simulations.

[8] This paper describes a numerical simulation of the Adriatic that was conducted with the Navy Coastal Ocean Model for this time period and a comparison of the results from the simulation with some of the ADCP and CTD observations. The main focus is the period of January–February 2003, during which several bora events occurred. The following sections include descriptions of (2) the ocean model, (3) the ocean model setup, (4) the observations used for validation of the model simulation, (5) the model results and comparison with observations, and (6) summary and conclusions.

2. Ocean Model

[9] The ocean model used here is the Navy Coastal Ocean Model (NCOM) as described by *Martin* [2000], with some improvements as described by *Morey et al.* [2003] and *Barron et al.* [2006]. This model is similar in its physics and numerics to the Princeton Ocean Model (POM) [*Blumberg and Mellor*, 1987], but uses an implicit treatment of the free surface and a hybrid vertical grid with sigma coordinates in the upper layers and (optionally) level coordinates below a user-specified depth. Only the sigma coordinate part of the grid moves with the free surface.

[10] The model equations include a source term that can be used for river inflows. There are options for higher-order treatment of some terms, for example, third-order upwind for advection [*Holland et al.*, 1998], which was used for the simulations conducted here. Vertical mixing is computed using the Mellor-Yamada Level 2 scheme [*Mellor and Yamada*, 1974], which is modified for use over the entire water column. The equation of state is that of *Mellor* [1991] as used in POM.

3. Ocean Model Setup

3.1. Ocean Model Domain

[11] The ocean model domain consists of the entire Adriatic Sea and includes the Strait of Otranto and a small part of the northern Ionian Sea. Three different computational grids have been used for the Adriatic modeling: a 3-km resolution grid with a 1-km nest in the northern Adriatic and single 2-km and 1-km resolution grids over the entire Adriatic. Comparison of results on the different grids have provided some indication of the sensitivity of the results to the model grid and bathymetry. Results presented here are from the 1-km grid covering the full Adriatic. Figure 1 shows the bathymetry for the entire domain covered by this grid and Figure 2 shows the bathymetry in the northern Adriatic in more detail. The bathymetry was derived from a database developed by the Naval Oceanographic Office and nautical chart soundings and the land-sea boundary was derived from the Generic Mapping Tools (GMT) vector shoreline.

Figure 1. Model domain and bathymetry.

[12] The vertical coordinate used with the 1-km grid consists of 32 total layers, with 22 sigma layers used from

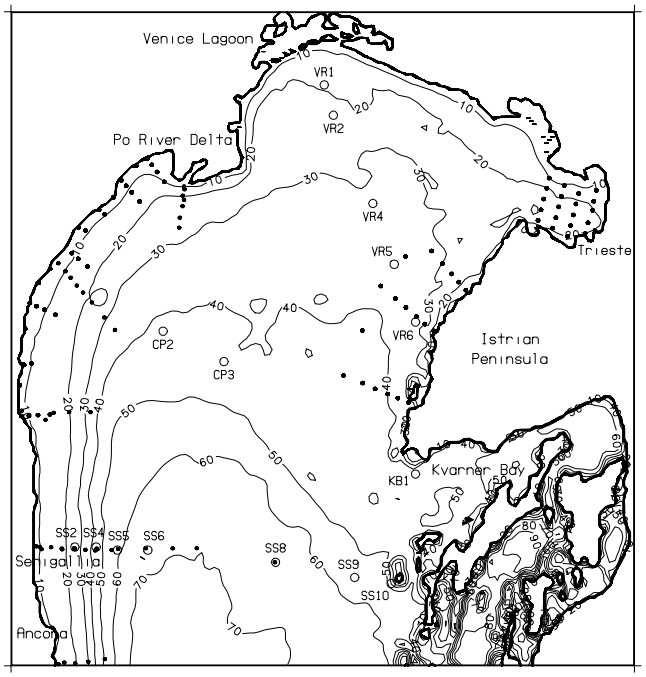

Figure 2. Model bathymetry in northern Adriatic (contour interval is 10 m) with mooring locations (labeled open circles) and locations of CTDs taken in January–February 2003 (small dots).

the surface down to a depth of 291 m and level coordinates used below 291 m. Hence the grid is like a regular sigma coordinate grid in water shallower than 291 m and is similar to a level grid in deeper water. The vertical grid uses a uniform stretching with a maximum thickness of the upper layer of 2 m and a maximum depth of 1262 m. The minimum bottom depth was set to 2 m.

3.2. Initial and Boundary Conditions

[13] Initial conditions (IC) for sea surface height (SSH), velocity, temperature (T), and salinity (S) were interpolated from a hindcast of the Naval Research Laboratory (NRL) global NCOM model [*Barron et al.*, 2004] for 00Z, 1 September 2002. Boundary conditions (BC) at the open boundary in the northern Ionian Sea were provided by daily values of SSH, velocity, T, and S from the global model. The numerical treatment of the BC includes the Flather radiative BC [*Flather and Proctor*, 1983] for the SSH and depth-averaged normal velocity, Orlanski radiation conditions [*Orlanski*, 1976] for the tangential velocities, T, and S, and a relaxation to the T and S fields of the global model near the open boundary. The normal baroclinic velocity at the open boundary is computed using the full model equation except that advection is only computed normal to the boundary using a first-order upwind scheme.

3.3. Tidal Forcing

[14] Tidal forcing was provided using tidal SSH and depth-averaged normal and tangential velocities at the open boundaries from the Oregon State University (OSU) tidal databases, which are derived from satellite altimetry data [*Egbert and Erofeeva*, 2003]. The tidal data are linearly added to the BC from global NCOM (which does not include tides). Data from the OSU Mediterranean tidal database were used for the K1, O1, M2, and S2 constituents and data from the OSU global database were used for P1, Q1, K2, and N2. Tidal potential forcing for these eight constituents was used in the interior of the model domain.

3.4. Atmospheric Forcing

[15] Atmospheric forcing was obtained from the atmospheric component of the Coupled Ocean-Atmosphere Mesoscale Prediction System (COAMPS™) [*Hodur*, 1997]. The COAMPS setup for the Adriatic consists of a triply nested grid with resolutions of 36, 12, and 4 km [*Pullen et al.*, 2003]. The outer grid of this nested grid system covers most of Europe and the Mediterranean and the inner 4-km grid covers the entire Adriatic and part of the Tyrhennian Sea. COAMPS itself is nested within the Navy Operational Global Atmospheric Prediction System (NOGAPS) [*Rosmond et al.*, 2002].

[16] Atmospheric forcing was provided by hourly fields of surface air pressure, wind stress, solar radiation, net longwave radiation, and precipitation from the COAMPS 4-km grid. Latent and sensible heat fluxes were computed with standard bulk formulas using the COAMPS 10-m wind speed and 2-m air temperature and humidity and the ocean model SST. The stability-dependent *Kondo* [1975] drag coefficient was used for the bulk flux calculations with neutral values of 0.0014 and 0.0011 for the latent and sensible heat fluxes, respectively. The evaporative moisture flux was derived from the bulk-calculated latent heat flux. The use of bulk formulas and the model SST to compute the latent and sensible heat fluxes provides an indirect relaxation to the SST analysis used for COAMPS. In addition, the ocean model SST was relaxed to the COAMPS SST analysis via a heat flux computed as the difference between the analysed SST and the ocean model SST multiplied by (a rate of) 1 m/d.

3.5. River and Runoff Inflows

[17] Rivers are input into the ocean model as a volume source with a specified vertical distribution, zero salinity, and a specified temperature. Since real-time river temperatures were not available, the river temperatures were specified from the monthly climatology for the Adriatic at the location of the river mouth. River and runoff inflows for the Adriatic were taken from the monthly climatological database of *Raicich* [1994]. This database includes discharges for about 39 rivers and runoff inflows along a number of sections of the Adriatic coastline. For input to the model, the runoff inflows were distributed along the appropriate part of the coast. The total annual mean discharge for the Adriatic from Raicich's database is about 5700 m^3/s. Daily observed discharge values were used only for the Po River (R. Signell, personal communication, 2003). The Po was input at 5 different locations with each location getting a fixed fraction of the total Po discharge.

3.6. Model Simulation

[18] The ocean model was run from 1 September 2002 to the end of March 2003 and model fields were saved every 3 hrs for analysis and comparison with observations. Additionally, hourly values of the model fields were saved at the mooring locations (Figure 2). The main focus of the results

Table 1. Model Tidal SSH Mean and RMS Errors Relative to IHO Stations

	Amplitude, cm		Phase, deg	
Tide	Mean	RMS	Mean	RMS
M2	−0.9	1.2	−5.3	8.5
K1	−1.2	1.5	5.3	7.0
S2	0.3	0.7	−15.1	16.5
P1	−1.0	1.3	32.0	35.0
O1	−0.1	0.5	−12.8	18.0
N2	0.6	0.9	17.8	26.4
K2	−0.3	0.4	42.5	42.9
Q1	0.1	0.1	−3.9	8.1

presented in this paper is the time period from the beginning of January to the end of February 2003.

4. Observations

[19] There were a large number of observations of different kinds taken during this experiment, and many of these are discussed in other papers in this special issue. In this paper, the ocean model results are mainly compared with some of the ADCP and CTD measurements.

[20] A number of ADCP moorings were deployed under the NRL Adriatic Circulation Experiment (ACE) together with the NATO Undersea Research Centre (NURC) as a Joint Research Project (JRP). The locations of these moorings are shown in Figure 2. There were 14 JRP moorings and an additional upward looking ADCP was mounted near the base of a meteorological tower [*Cavaleri*, 2000]. The JRP moorings consisted of trawl-resistant, bottom-mounted ADCPs [*Perkins et al.*, 2000]. All of these moorings measured bottom temperature and pressure and three of the moorings also measured bottom salinity. The ADCPs measured currents within the water column from a distance of about 3 m above the bottom to about 5 m below the surface.

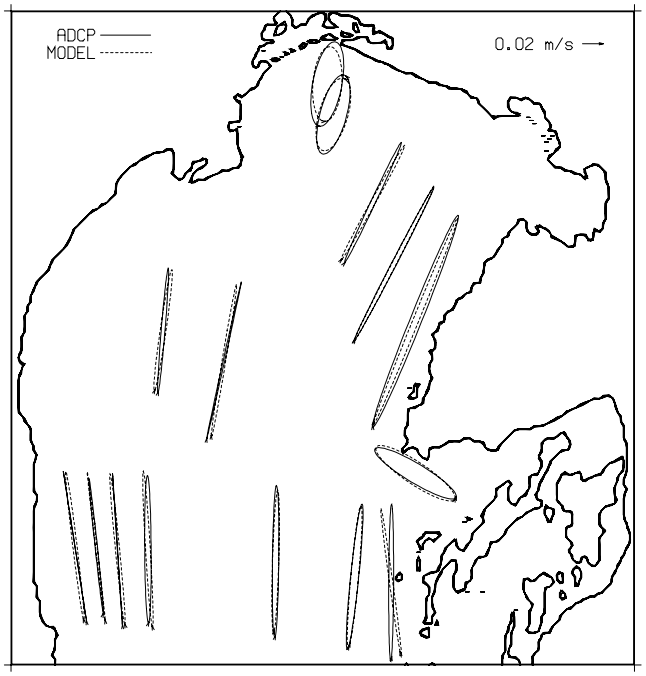

Figure 3. Model and ADCP M2 tidal ellipses at 10 m.

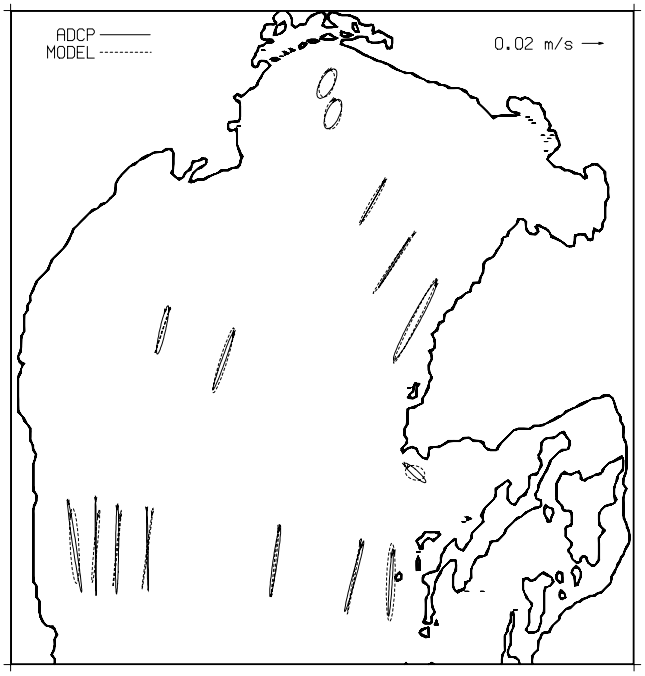

Figure 4. Model and ADCP K1 tidal ellipses at 10 m.

[21] The currents observed at VR5 were in fairly good agreement with the model currents except for the direction. The disagreement in the direction was especially noticeable in the tidal ellipses, which were rotated about 30° counterclockwise relative to the tidal ellipses predicted by NCOM and other models (M. Kuzmic, personal communication, 2004) and derived from drifters (P. Poulain, personal communication, 2005). Investigation of the VR5 mooring data did not reveal a reason for the discrepancy. Because of these direction discrepancies, the VR5 currents were rotated 30° clockwise for all the comparisons performed in this paper.

[22] The CTD data were collected during several cruises funded by the ADRICOSM, EuroSTRATAFORM, and

Table 2. Percent of Total Current Variance Due to Tides at Mooring Locations

	5-m Depth		Near Bottom	
Name	Model	ADCP	Model	ADCP
SS2	17.2	16.8	25.5	20.6
SS4	16.8	15.1	31.9	18.7
SS5	21.5	18.3	35.7	29.4
SS6	28.1	23.0	43.5	36.4
SS8	30.5	24.5	46.7	39.0
SS9	33.2	24.8	46.0	32.4
SS10	36.8	31.2	40.4	34.6
KB1	5.8	9.7	15.1	18.2
CP2	17.6	17.5	40.5	34.6
CP3	25.3	29.5	47.4	42.0
VR1	9.7	10.1	11.6	13.7
VR2	12.3	9.7	20.0	13.3
VR4	22.7	20.1	37.0	35.7
VR5	38.5	30.1	51.9	39.4
VR6	61.5	53.4	69.7	61.2

Table 3. Model Mean, RMS, and Correlation Errors With Respect to ADCP Measured Velocities at 10 m[a]

	Principal Axis			Minor Axis		
Name	Mean	RMS	Cor	Mean	RMS	Cor
SS2	4.9	13.0	0.601	−0.1	5.5	−0.088
SS4	0.1	8.2	0.811	−0.1	5.4	0.031
SS5	2.0	8.3	0.732	−0.9	5.2	0.065
SS6	5.0	8.8	0.683	−3.9	7.8	−0.114
SS8	0.4	5.9	0.694	−3.5	7.4	0.217
SS9	−1.4	5.9	0.665	−4.5	7.6	0.329
SS10	4.1	8.4	0.533	−0.5	4.7	0.448
KB1	−16.2	23.2	0.248	3.0	9.6	0.111
CP2	−3.4	9.3	0.164	1.5	6.7	0.051
CP3	−3.5	9.0	0.499	−1.8	5.8	0.153
VR1	−4.0	9.2	0.654	−0.3	4.3	0.034
VR2	−0.6	7.3	0.645	−0.2	3.6	0.100
VR4	1.9	10.3	0.288	−2.5	6.0	0.094
VR5	−0.9	7.3	0.621	−0.8	5.7	−0.059
VR6	0.6	7.6	0.275	2.3	4.0	0.475

[a]Velocities are detided. Errors are computed along the local principal and minor variance axes. Mean and RMS errors are in cm/s.

ACE projects. The locations of the CTDs taken during January–February 2003 in the northern Adriatic are shown in Figure 2.

5. Results

5.1. Tidal Sea Surface Height

[23] The model tidal SSH was compared with data from 27 International Hydrographic Organization (IHO) stations. These included all the IHO stations in the Adriatic except those in Venice Lagoon (Venice Lagoon is not adequately resolved by the model grid and the tides are not properly simulated there). A harmonic analysis of the model tides was performed using least squares fitting to the 8 tidal constituents used for the tidal forcing.

[24] The tidal SSH mean and root mean square (rms) errors with respect to the IHO stations are listed in Table 1.

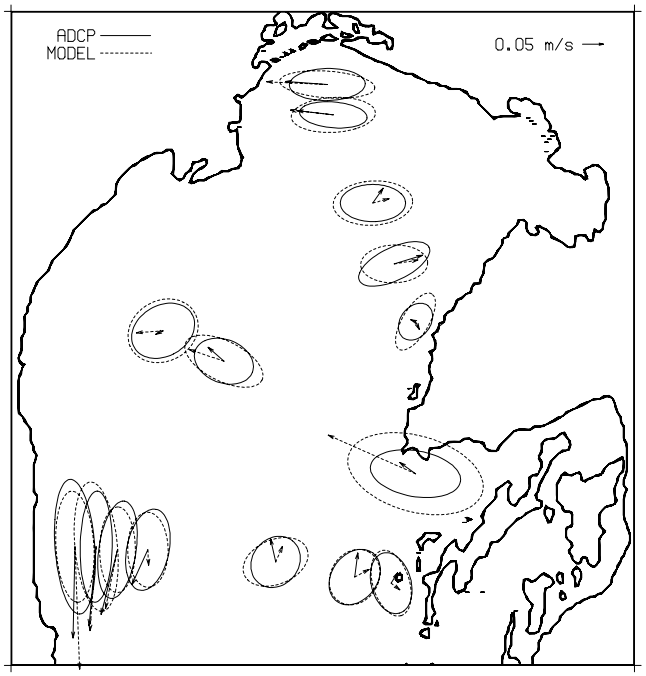

Figure 5. Detided model and ADCP mean current vectors and std current ellipses at 5 m.

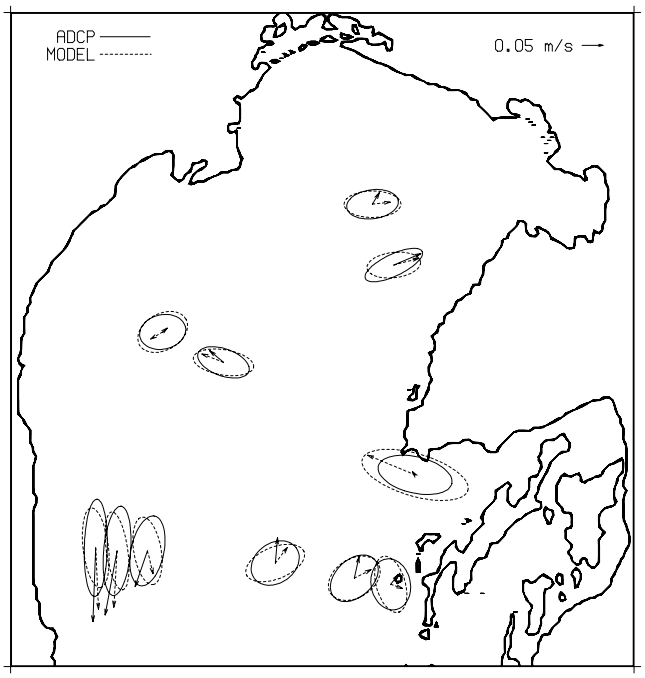

Figure 6. Detided model and ADCP mean current vectors and std current ellipses at 30 m.

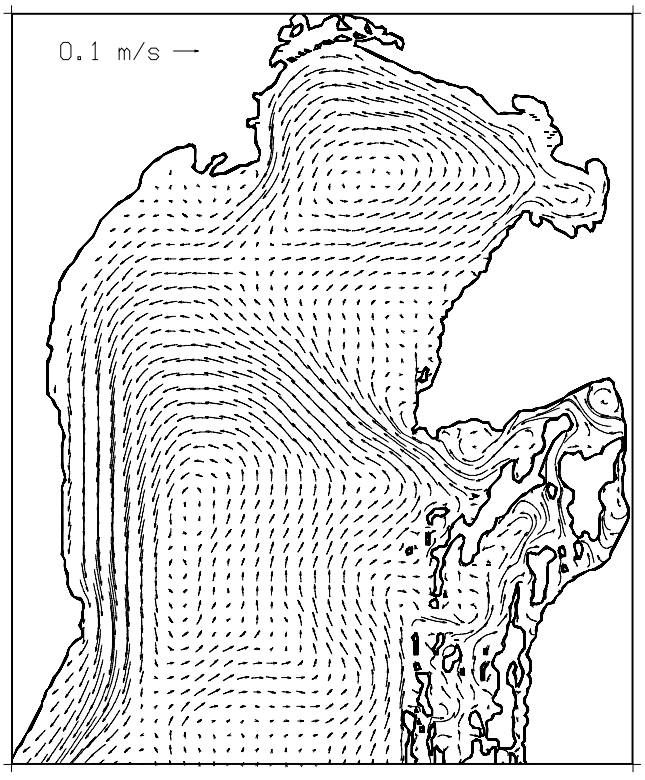

Figure 7. Model mean currents for January–February at 5 m.

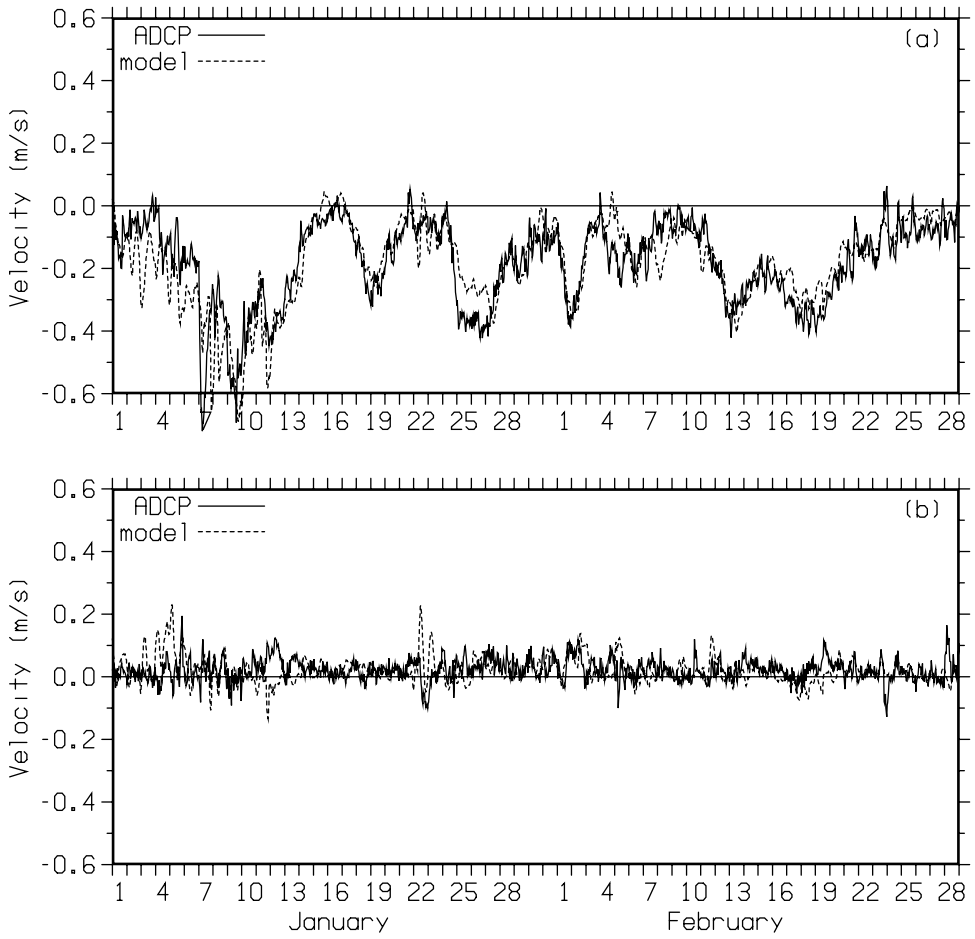

Figure 8. Detided model and ADCP 10-m currents at SS4 for January–February along axes of (a) maximum and (b) minimum variance.

For the largest tide, M2, the mean and rms errors for the amplitude were −0.9 and 1.2 cm, respectively, and the mean and RMS errors for the phase were −5.3° and 8.5°. The large size of the mean errors relative to the RMS errors for some of the constituents suggests that a uniform adjustment of the amplitude and phase of the tidal boundary forcing could significantly reduce the differences.

[25] Several single-layer, barotropic tidal simulations were performed on the 1-km grid to investigate the relative importance of the tidal potential forcing. Turning off the tidal potential reduced the M2 tidal amplitude in the northern Adriatic about 12%, e.g., the M2 amplitude at Trieste decreased from 26.1 to 23.0 cm. Turning off the tidal potential reduced the K1 and S2 tides by about 7 and 8%, respectively.

5.2. Tidal Currents

[26] Tidal currents for the main tidal constituents were computed from the mooring data and from the model results at the mooring locations using least squares fitting. Figures 3 and 4 show plots of the model and mooring M2 and K1 tidal current ellipses. There is fairly good agreement in the amplitude and orientation of the tidal ellipses at all the mooring locations that were used (the direction of the currents at VR5 was modified as discussed in Section 4). The tidal currents for the K1 and O1 constituents also agree well with the mooring currents. The fraction of the total variance of the ADCP currents due to the tides (Table 2) ranges from a low of 10% near the surface at KB1 to 64% near the bottom at VR6.

5.3. Detided Currents

[27] Table 3 lists error statistics for the difference between the model-predicted and ADCP currents at the moorings for January–February at 10-m depth. For all the results presented in this section, the model and ADCP currents were detided by subtracting the least squares fit tidal currents.

[28] Figures 5 and 6 show plots of the 5-m and 30-m mean current vectors and standard deviation (std) ellipses for the model and ADCP currents at the mooring locations for January–February. Note that the scaling of the std ellipses is smaller than for the plots of the tidal ellipses in Figures 3 and 4 by a factor of 2.5.

[29] The mean currents in the alongshore WAC off Senigallia and Venice Lagoon are in good agreement with the ADCP data. There are significant discrepancies at some of the other locations. The largest discrepancy is at KB1 where the model shows a much larger mean flow out of Kvarner Bay than was observed. The model currents at KB1 are generally out of the bay, whereas the observed currents

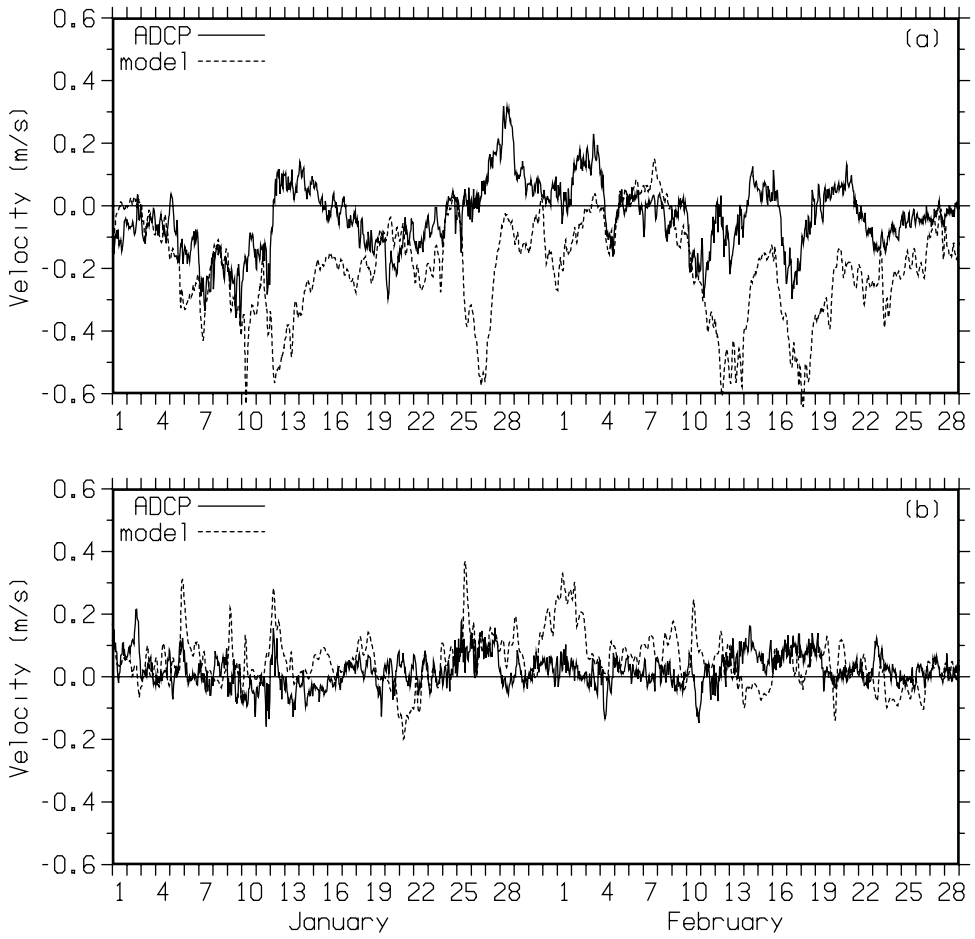

Figure 9. Detided model and ADCP 10-m currents at KB1 for January–February along axes of (a) maximum and (b) minimum variance.

are more evenly divided between outflowing and inflowing currents.

[30] The model currents at SS8 and SS9 just south of Kvarner Bay are more directed toward the mouth of the Bay than the observed currents.

[31] The model mean currents are in good agreement with the observed mean currents at VR5 in both magnitude and direction, which supports the decision to correct the direction of the VR5 currents.

[32] The magnitude and orientation of the std ellipses of the model currents are generally in good agreement with those of the observed currents. The largest discrepancy is again at KB1 where the std of the model currents is about 50% larger than that of the observed currents.

[33] Figure 7 shows the model mean currents for January–February at 10-m depth. The mean circulation during this period mainly reflects the model's mean response to bora with two large cyclonic cells in the northern Adriatic separated by a wedge of weaker currents near Istria.

[34] Figure 8 shows a comparison of the 10-m model and ADCP velocities at SS4 for January–February. The currents are plotted as components along the axes of maximum and minimum variance, which for SS4 (and many of the other mooring locations) correspond roughly to the alongshore and cross-shore directions, respectively, as shown in Figures 5 and 6. The model captures the longer-timescale (multiday) events in the WAC fairly well. These events are bora-induced intensifications of the WAC similar to those described by *Book et al.* [2005] for the winter of 2001. However, there is less correspondence between short-timescale events in the model and the ADCP observations of the WAC. Along the axis of minimum variance, the magnitude and timescale of the current fluctuations tend to be small and Table 3 indicates that there is little correlation between the model and ADCP currents along this axis at many of the moorings.

[35] Figure 9 shows a comparison of the 10-m model and ADCP velocities at KB1. The model shows outflow from Kvarner Bay most of the time and strong outflow during bora events. In contrast, the observed current is often directed into Kvarner Bay and tends to be weaker during boras. The model response for simulations that were run on different grids with slightly different bathymetries (section 3.1), was similar to the model response shown here, which suggests that the problem is not due to the specific geometry of the ocean model grid that was used. It may that that there is a problem with the location and/or structure of the bora wind jets over

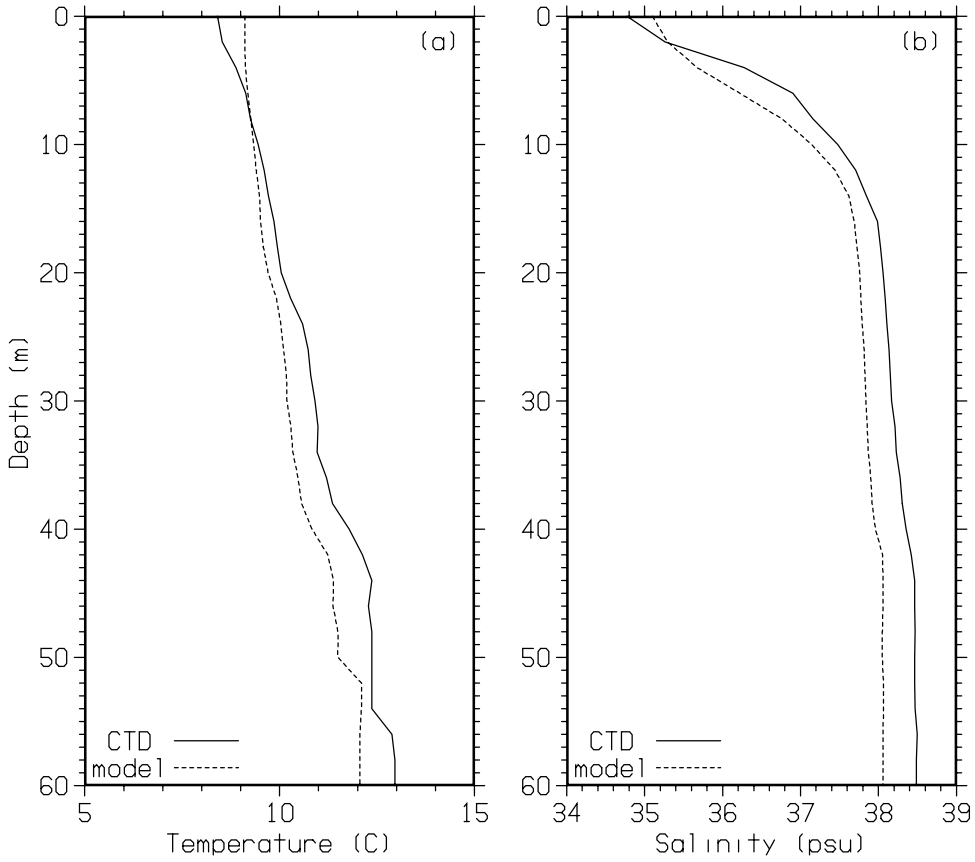

Figure 10. Model and CTD mean (a) temperature and (b) salinity profiles for January–February.

Kvarner Bay predicted by COAMPS. This discrepancy needs further investigation.

5.4. Comparison With CTD Observations

[36] A large number of CTD profiles were taken in the northern Adriatic during ACE. Figure 10 shows the mean and Figure 11 the std of 345 T and S profiles from the CTD observations (Figure 2) and from the model simulation during January–February. For this comparison, the model T and S fields were interpolated to the location and time of the CTDs. Figure 12 shows the RMS differences between the model and CTD T and S profiles.

[37] The increase of the mean temperature with depth for both the model and the CTD observations (Figure 10) reflects the colder water in the shallower regions as well as temperature inversions caused by surface cooling and the stabilizing effect of the low-salinity water from the rivers near the surface in some areas. There is a cold bias of 0.5 to 1°C in the model temperatures below 20 m. The model captures the mean increase of salinity with depth in the upper 15 m quite well, but the model has a low-salinity bias of 0.2 to 0.4 psu at depths below 5 m.

[38] The std of the model temperature profiles is similar to that of the CTDs below 30 m, but between 30 m and the surface the difference steadily increases, with the model std being lower. The lower std of the model temperature near the surface is probably at least partly due to the relaxation of the model SST to the COAMPS SST analysis. The SST analysis was fairly smooth and hence tended to suppress variability in the model near-surface temperature.

[39] The std of the model salinity profiles agrees very well with that of the CTDs (Figure 11). This and the good agreement of the shape of the mean salinity profiles (Figure 10) suggests that the model freshwater inflows into the Adriatic result in a realistic vertical salinity structure, with most of the variability of salinity due to the freshwater discharges being contained within the upper 15 m.

[40] The small RMS error of the model salinity (Figure 12) relative to the salinity std (Figure 11) and the high index of agreement [*Willmott et al.*, 1985] of 0.85 for the model and observed salinity in the upper 10 m indicate that the model simulation shows skill in predicting the horizonal variability of salinity structure due to the freshwater inflows.

[41] The model RMS error relative to the CTDs is about 1°C for temperature and about 0.4 psu for salinity below 15 m. A large part of this RMS error is due to the model's low-temperature and low-salinity biases.

5.5. Model Heat Budget for Northern Adriatic

[42] A heat budget for January–February was computed for the model for the region of the Adriatic north of the SS mooring line (Figure 2). The mean temperature of this region decreased about 4.1°C during the two months. The effective temperature decrease due to surface heat fluxes was 6.3°C (which is equivalent to a mean surface heat flux of about 175 W/m^2), and this was partially offset by a mean increase in temperature due to advection and river inflows

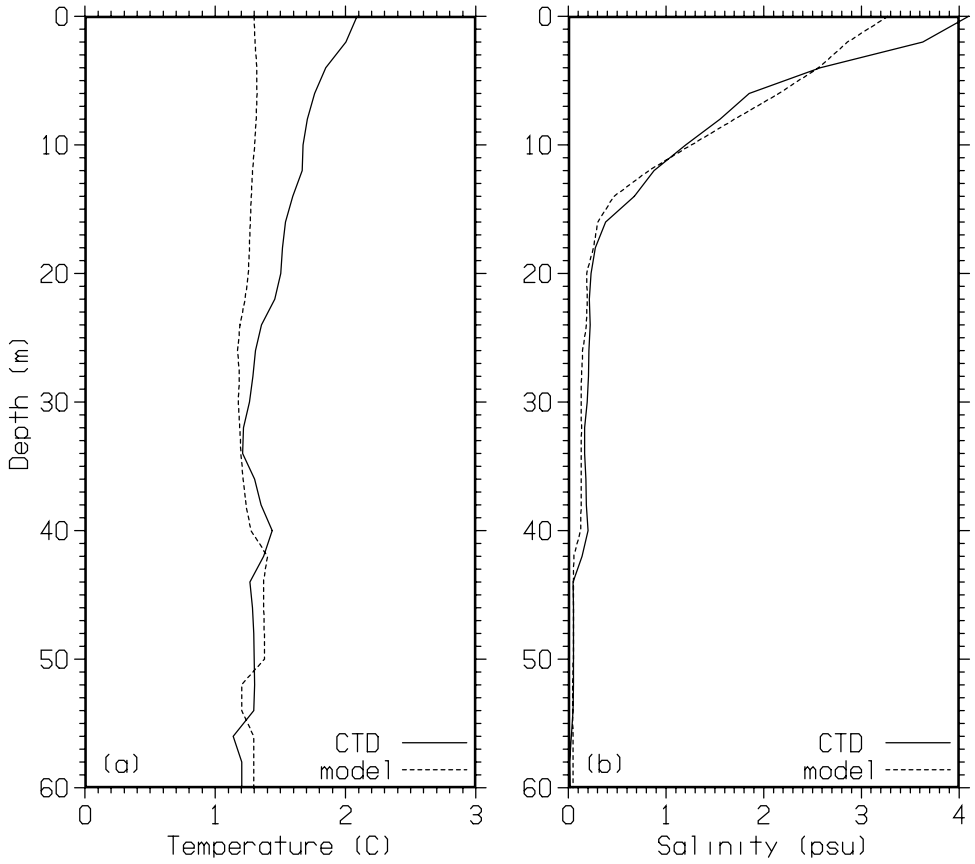

Figure 11. Model and CTD (a) temperature and (b) salinity std profiles for January–February.

of 2°C and 0.2°C, respectively. The use of proper river inflow temperatures would likely have led to a net cooling from the rivers, rather than a slight warming.

5.6. Bora Response

[43] The effect of the winds and wind stress curl during bora events has been noted by a number of investigators [*Orlic et al.*, 1994; *Rachev and Purini*, 2001; *Beg Paklar et al.*, 2001]. The variations in the mountain topography of Croatia act to force the bora winds out over the water in strong jets and set up a wind stress pattern that tends to recur during different bora events with variations mainly in amplitude and duration.

[44] The COAMPS winds used for the model simulations here have sufficient resolution (4 km) to respond to the main features of the orography along the Croatian coast and provide a fairly realistic pattern of strong, separated jets [*Pullen et al.*, 2003]. Figure 13 shows a plot of the COAMPS 24-hour-averaged wind stress during the bora of 12 January.

[45] Figure 14 shows the model response to the bora that occurred on 12 January. The response to this bora by the ocean model simulations run on other computational grids was very similar, and other bora events during the winter of 2003 generated similar circulation patterns.

[46] Figure 14 shows large, cyclonic gyres in the north-central and northern Adriatic and a smaller anticyclonic gyre near the Istrian Peninsula between the large cyclonic gyres. This double-gyre pattern is consistent with past theoretical and modeling studies and the JRP data offer clear evidence for the existence of the two strong cyclonic cells.

[47] The model response to the bora of 12 January produces circulations in the southern half of Figure 14 that depart significantly from the classic view of a large-scale cyclonic circulation framed by the WAC and the EAC. The WAC is present all along the Italian coast, but a significant portion of its southeastward flow north of Ancona recirculates toward Croatia forming a tighter cyclone. Below this cyclone, the EAC has been replaced by a small cyclone–anticyclone pair. Hence, during this time period of intense wind, there are five separate semiclosed cells in the northern Adriatic.

[48] The closing of the two most southern cells is transient. The less frequent of these two cells is the more southerly, cyclonic cell. However, this cell appears in the model simulation at least once (though usually briefly) during each of the five bora that occurred during January–February. When these gyres are not present during bora winds, there are frequently corresponding cyclonic and anticyclonic meanders in the EAC and these meanders are persistent enough to be preserved in the January–February mean field (Figure 7).

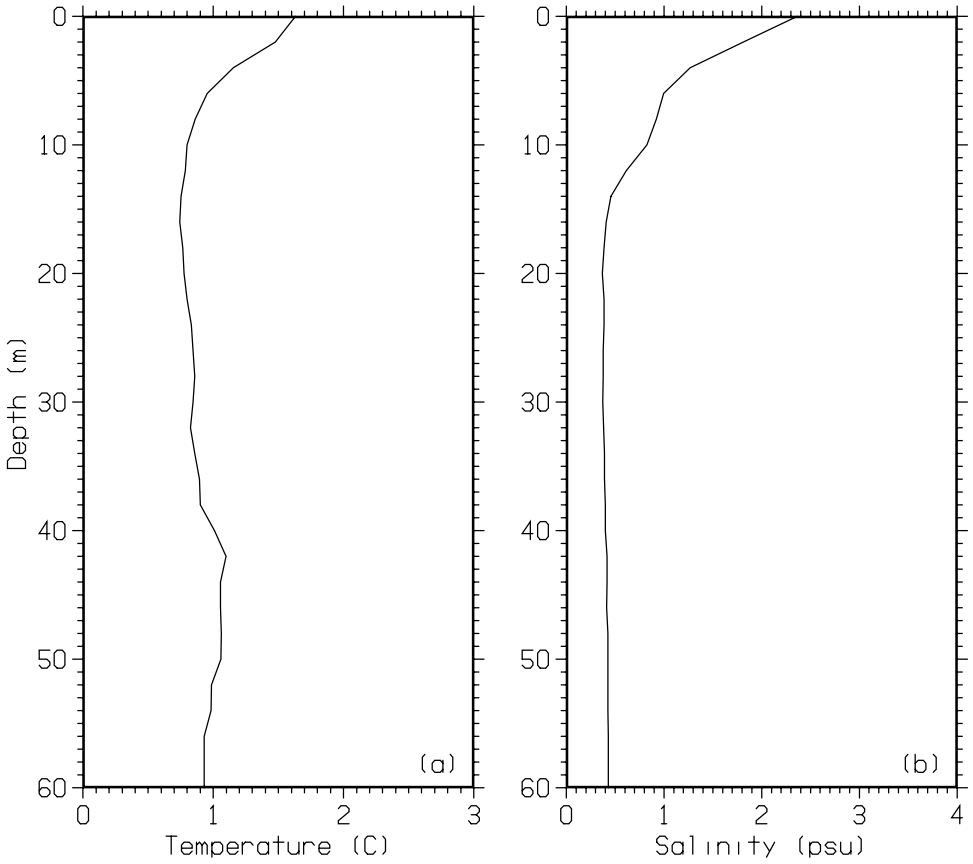

Figure 12. Model and CTD RMS (a) temperature and (b) salinity profile differences for January–February.

[49] Unfortunately, the measurements taken during this period were not located in optimal positions for validating the tight recirculation, the meanders of the EAC, and the closing of these meanders to form the separate cyclonic and anticyclonic cells that are observed in the model simulations. However, the data do present some evidence in support of these features. At the start of each strong bora period, the observed barotropic velocities at mooring SS8 have significant flow toward Croatia. That is, velocities are briefly directed approximately toward 5°T rather than toward −40°T. During bora, the shear in the alongshore velocity component between moorings SS10 and SS9 peaks in an anticlockwise sense. This result supports the model-simulated anticyclonic cell or meander in the EAC south of these positions. ADCP measurements made by the EACE program [*Orlic et al.*, 2006] show cyclonic-type shear in the EAC for January and February. The southernmost cyclonic cell in Figure 14 is positioned at the sites of these two moorings, and thus this shear lends support to the predictions of a cyclonic meander or cell. However, peaks in shear between these positions from the data or from the model do not show the same level of correlation with bora events as the results from SS10 and SS9.

[50] Figure 15 shows a plot of the COAMPS wind stress curl averaged over the 24 h preceeding the circulation snapshot shown in Figure 14. The areas of positive and negative wind stress curl match the regions of cyclonic and anticyclonic circulation in Figure 15 and show the strong control exerted by the winds on the circulation during these events.

6. Summary and Conclusions

[51] The NCOM-modeled tidal height shows good agreement with IHO stations in the Adriatic and the modeled tidal current ellipses show good agreement with ADCP measurements. The fraction of the total current variance due to the tides at the mooring locations at 5-m depth ranges from 6 to 70%.

[52] Comparison of detided model and ADCP currents at 10-m depth for January–February shows RMS errors along the principal variance axes ranging from 6 to 12.9 cm/s and correlations ranging from 0.16 to 0.81. Correlations between the detided model and ADCP currents along the minor variance axes are generally low.

[53] In general, the model predicts longer-timescale features well at all the JRP locations except at KB1. The lack of model-to-data correlation between shorter-timescale features and minor variance axis flows may be due to the presence of small-scale eddies and instabilities. The phasing and location of such features may not be very deterministic as demonstrated by the sensitivity of these features to the different ocean model grids used in this study. The disagreement between the model and the measurements at KB1 requires further study and explanation.

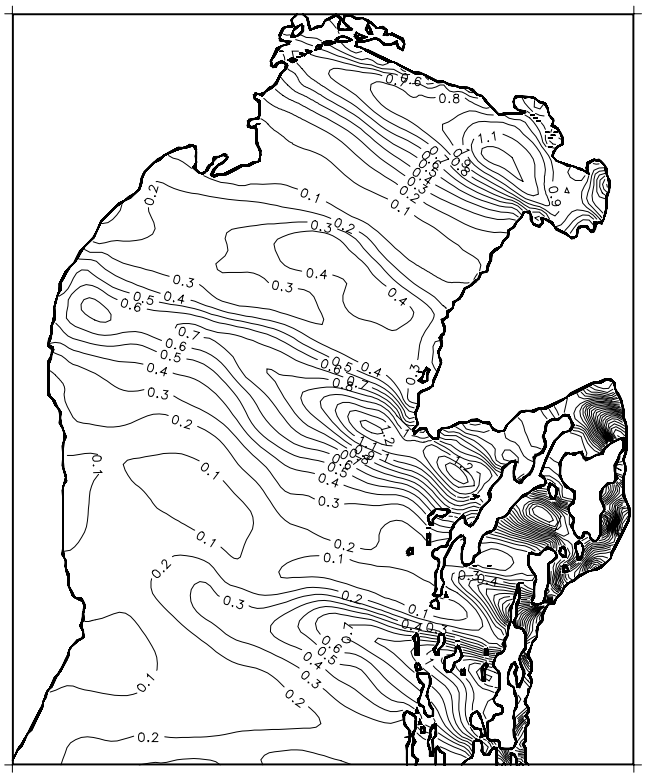

Figure 13. Time-averaged COAMPS wind stress for period 09Z, 11 January, to 09Z, 12 January 2003. Contour interval is 0.1 Pa.

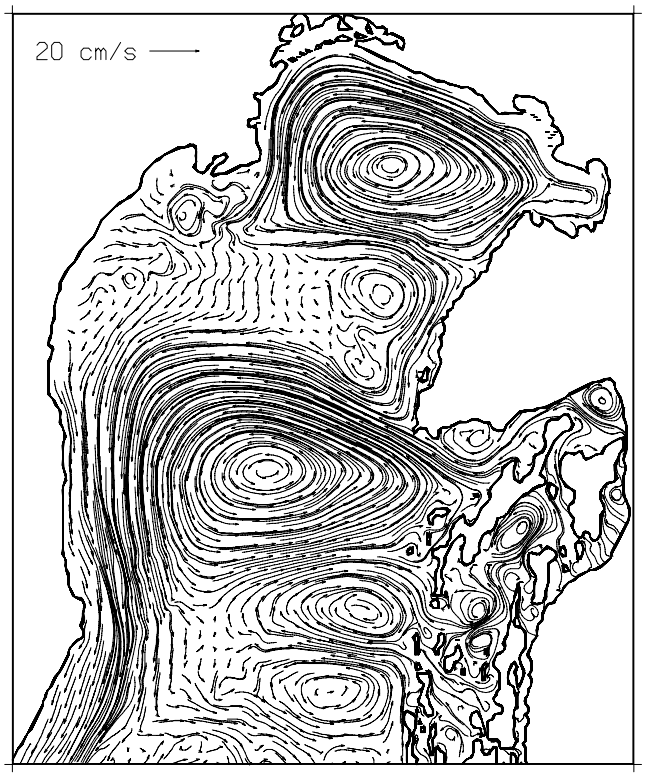

Figure 14. Model 10-m currents at 09Z, 12 January 2003.

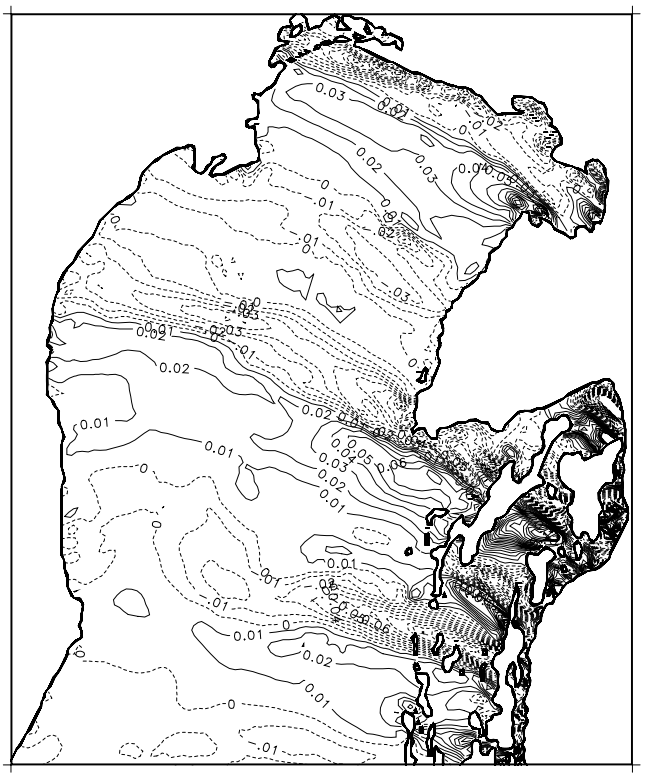

Figure 15. Time-averaged COAMPS wind stress curl for period 09Z, 11 January, to 09Z, 12 January 2003. Contour interval is 0.01 Pa/km.

[54] Comparison of the model-simulated temperature and salinity profiles during January–February with CTD measurements indicate that the model captures some of the spatial structure of the observed fields. The good agreement of the model and observed salinity mean and std and the high (0.85) index of agreement of the model salinity with the observed salinity in the upper 10 m indicate that the model freshwater inflows into the Adriatic result in a realistic vertical salinity structure and that the model has some skill in predicting horizontal salinity variations. The model shows a bias of about -1°C below 20 m and -0.2 to -0.4 psu relative to the CTDs.

[55] The model response to the several bora events in January–February shows a recurring pattern of large cyclonic and smaller anticyclonic gyres that generally agree with the ADCP observations and reflect the pattern of wind stress curl from the COAMPS wind stress forcing. During strong bora forcing, two large cyclonic circulation gyres form in the northern Adriatic with a smaller anticyclonic circulation between them near the Istrian Peninsula. Southeast of Kvarner Bay, a couple of relatively large meanders frequently occur within the Eastern Adriatic Current (EAC) and these meanders sometimes close to form small cells. The circulation within the meander/cell closer to Kvarner Bay is anticyclonic and the more southeasterly meander/cell is cyclonic.

[56] **Acknowledgments.** Thanks to Hank Perkins for planning and leading the ACE project. Thanks to Mark Hulbert and Ray Burge of NRL and the technical team of NURC for their work in the successful deployment and recovery of all the JRP moorings. Thanks to Rich Signell and

NURC for their willingness to allow us to use NURC data for this publication. Thanks to the ADRICOSM and EuroSTRATAFORM projects for sharing CTD data and to Aniello Russo of the Polytechnic University of Marche for his work to organize some of these data. Thanks to the EACE program and the University of Zagreb, the Institute of Oceanography and Fisheries, and the Hydrographic Institute of the Republic of Croatia for sharing their ADCP data. This work was supported by the Office of Naval Research as part of the research programs "Adriatic Circulation Experiment" and "Dynamics of the Adriatic in Real-Time" under Program Element 0602435N and by the NRL "Mountain Wave Dynamics" Project under Program Element 0601153N. COAMPS® is a registered trademark of the Naval Research Laboratory. This is NRL contribution NRL/JA/7320–05-5290.

References

Artegiani, A., D. Bregant, E. Paschini, N. Pinardi, F. Raicich, and A. Russo (1997a), The Adriatic Sea general circulation. part I: Air-sea interaction and water mass structure, *J. Phys. Oceanogr.*, *27*, 1492–1514.

Artegiani, A., D. Bregant, E. Paschini, N. Pinardi, F. Raicich, and A. Russo (1997b), The Adriatic Sea general circulation. part II: Baroclinic circulation structure, *J. Phys. Oceanogr.*, *27*, 1515–1532.

Barron, C. N., A. B. Kara, H. E. Hurlburt, C. Rowley, and L. F. Smedstad (2004), Sea surface height predictions from the global Navy Coastal Ocean Model (NCOM) during 1998–2001, *J. Atmos. Oceanic Technol.*, *21*, 1876–1894.

Barron, C. N., A. B. Kara, P. J. Martin, R. C. Rhodes, and L. F. Smedstad (2006), Formulation, implementation and examination of vertical coordinate choices in the global Navy Coastal Ocean Model (NCOM), *Ocean Modell.*, *11*, 347–375, doi:10.1016/j.ocemod.2005.01.004.

Beg Paklar, G. B., V. Isakov, D. Koracin, V. Kourafalou, and M. Orlic (2001), A case study of bora-driven flow and density changes on the Adriatic shelf (January, 1987), *Cont. Shelf Res.*, *21*, 1751–1783.

Blumberg, A. F., and G. L. Mellor (1987), A description of a three-dimensional coastal ocean circulation model, in *Three-Dimensional Coastal Ocean Models*, *Coastal Estuarine Ser.*, vol. 4, edited by N. Heaps, pp. 1–16, AGU, Washington, D. C.

Book, J. W., H. T. Perkins, L. Cavaleri, J. D. Doyle, and J. D. Pullen (2005), ADCP observations of the western Adriatic slope current during winter of 2001, *Prog. Oceanogr.*, *66*, 270–286, doi:10.1029/2003JC001780.

Cavaleri, L. (2000), The oceanographic tower Acqua Alta—Activity and prediction of sea states at Venice, *Coastal Eng.*, *39*, 29–70.

Cushman-Roisin, B., M. Gacic, P. Poulain, and A. Artegiani (2001), *Physical Oceanography of the Adriatic Sea: Past, Present, and Future*, 304 pp., Springer, New York.

Egbert, G. D., and S. Y. Erofeeva (2003), Efficient inverse modeling of barotropic ocean tides, *J. Atmos. Oceanic Technol.*, *19*, 183–204.

Flather, R. A., and R. Proctor (1983), Prediction of North Sea storm surges using numerical models: Recent developments in the U. K., in *North Sea Dynamics*, edited by J. Sundermann and W. Lenz, pp. 299–317, Springer, New York.

Hendershott, M. C., and P. Rizzoli (1976), The winter circulation in the Adriatic Sea, *Deep Sea Res.*, *23*, 353–370.

Hodur, R. M. (1997), The Naval Research Laboratory's Coupled Ocean/Atmosphere Mesoscale Prediction System (COAMPS), *Mon. Weather Rev.*, *125*, 1414–1430.

Holland, W. R., J. C. Chow, and F. O. Bryan (1998), Application of a third-order upwind scheme in the NCAR ocean model, *J. Clim.*, *11*, 1487–1493.

Hopkins, T. S., A. Artegiani, C. Kinder, and R. Pariante (1999), A discussion of the northern Adriatic circulation and flushing as determined from the ELNA hydrography, in *The Adriatic Sea*, *Ecosyst. Res. Rep. 32*, edited by T. S. Hopkins et al., pp. 85–106, Eur. Comm., Brussels.

Jiang, Q., and J. D. Doyle (2005), Wave breaking induced surface wakes and jets observed during a bora event, *Geophys. Res. Lett.*, *32*, L17807, doi:10.1029/2005GL022398.

Klemp, J. B., and D. R. Durran (1987), Numerical modeling of Bora winds, *Meteorol. Atmos. Phys.*, *36*, 215–227.

Kondo, J. (1975), Air-sea bulk transfer coefficients in diabatic conditions, *Boundary Layer Meteorol.*, *9*, 91–112.

Lee, C. M., et al. (2005), Northern Adriatic response to a wintertime bora wind event, *Eos Trans. AGU*, *86*, 157, 163, 165.

Martin, P. J. (2000), A description of the Navy Coastal Ocean Model Version 1.0, *NRL Rep. NRL/FR/7322–00-9962*, 42 pp., Nav. Res. Lab., Stennis Space Cent., Miss.

Mellor, G. L. (1991), An equation of state for numerical models of oceans and estuaries, *J. Atmos. Oceanic Technol.*, *8*, 609–611.

Mellor, G. L., and T. Yamada (1974), A hierarchy of turbulence closure models for planetary boundary layers, *J. Atmos. Sci.*, *31*, 1791–1806.

Morey, S. L., P. J. Martin, J. J. O'Brien, A. A. Wallcraft, and J. Zavala-Hidalgo (2003), Export pathways for river discharged fresh water in the northern Gulf of Mexico, *J. Geophys. Res.*, *108*(C10), 3303, doi:10.1029/2002JC001674.

Orlanski, I. (1976), A simple boundary condition for unbounded hyperbolic flows, *J. Comput. Phys.*, *21*, 251–269.

Orlic, M., M. Gacic, and P. E. La Violette (1992), The currents and circulation of the Adriatic Sea, *Oceanol. Acta*, *15*, 109–124.

Orlic, M., M. Kuzmic, and Z. Pasaric (1994), Response of the Adriatic Sea to the bora and sirocco forcing, *Cont. Shelf Res.*, *14*, 91–116.

Orlic, M., et al. (2006), Wintertime buoyancy forcing, changing seawater properties, and two different circulation systems produced in the Adriatic, *J. Geophys. Res.*, doi:10.1029/2005JC003271, in press.

Perkins, H., F. de Strobel, and L. Gualdesi (2000), The Barny sentinel trawl-resistant ADCP bottom mount: Design, testing, and application, *IEEE J. Oceanic Eng.*, *25*, 430–436.

Poulain, P. (2001), Adriatic Sea surface circulation as derived from drifter data between 1990 and 1999, *J. Mar. Syst.*, *29*, 3–32.

Pullen, J., J. D. Doyle, R. Hodur, A. Ogston, J. W. Book, H. Perkins, and R. Signell (2003), Coupled ocean-atmosphere nested modeling of the Adriatic Sea during winter and spring 2001, *J. Geophys. Res.*, *108*(C10), 3320, doi:10.1029/2003JC001780.

Rachev, N., and R. Purini (2001), The Adriatic response to bora forcing: A numerical study, *Nuovo Cimento Soc. Ital. Fis. C*, *24*, 303–311.

Raicich, R. (1994), Note on the flow rates of the Adriatic rivers, *Tech. Rep. RF 02/94*, 8 pp., Cons. Naz. delle Ric. Inst. Sper. Talassografico, Trieste, Italy.

Rosmond, T. E., J. Teixeira, M. Peng, T. F. Hogan, and R. Pauley (2002), Navy Operational Global Atmospheric Prediction System (NOGAPS): Forcing for ocean models, *Oceanography*, *15*, 99–108.

Smith, R. B. (1987), Aerial observations of the Yugoslavian bora, *J. Atmos. Sci.*, *44*, 207–269.

Willmott, C. J., S. G. Ackleson, R. E. Davis, J. J. Feddema, K. M. Klink, D. R. Legates, J. O'Donnell, and C. M. Rowe (1985), Statistics for the evaluation and comparison of models, *J. Geophys. Res.*, *90*, 1995–9005.

Zavatarelli, M., N. Pinardi, V. H. Kourafalou, and A. Maggiore (2002), Diagnostic and prognostic model studies of the Adriatic Sea general circulation: Seasonal variability, *J. Geophys. Res.*, *107*(C1), 3004, doi:10.1029/2000JC000210.

Zore-Armanda, M., M. Bone, V. Dadic, M. Gacic, V. Kovacevic, and Z. Vucak (1996), Ecological study of gas fields in the northern Adriatic, 4. Circulation, *Acta Adraitica*, *37*, 35–68.

J. W. Book, Ocean Sciences Branch, Oceanography Division, Naval Research Laboratory, Stennis Space Center, MS 39529, USA. (book@nrlssc.navy.mil)

J. D. Doyle, Atmospheric Dynamics and Prediction Branch, Marine Meteorology Division, Naval Research Laboratory, 7 Grace Hopper Ave., Monterey, CA 93943, USA. (doyle@nrlmry.navy.mil)

P. J. Martin, Ocean Dynamics and Prediction Branch, Oceanography Division, Naval Research Laboratory, Stennis Space Center, MS 39529, USA. (paul.martin@nrlssc.navy.mil)